# Quantum resource degradation theory within the framework of observational entropy decomposition

Xiang Zhou $^{*1,2}$ 

Received: date / Accepted: date

Abstract In quantum resource theories, traditional scalar measures often fail to capture the evolution of the quality of a resource under free operations. To address this limitation, we propose a quantum resource degradation theory based on the decomposition of observational entropy. We demonstrate that the total inconsistency measure,  $\mathcal{O}_{\mathcal{C}}$ , can be decomposed into two independent components: inter-block coherence,  $\mathcal{C}_{\rm rel}$ , and intra-block noise,  $\mathcal{D}_{\rm rel}$ . This decomposition reveals a significant degradation mechanism: under specific free operations, quantum coherence degrades into classical noise. Consequently, even when the total resource quantity is conserved, its quality decreases. This is quantified by the resource purity metric,  $\eta$ . Our theory provides greater detail than conventional approaches that rely solely on monotonicity. It also establishes a new framework for understanding quantum resource dynamics. We validate the theory through numerical experiments on Variational Quantum Algorithms (VQAs), demonstrating its utility in diagnosing and explaining the barren plateau phenomenon (BPP). The proposed framework establishes a new paradigm for managing resource quality, complementing traditional resource quantification. This contributes to the optimization of quantum technologies on current and near-term noisy quantum devices.

**Keywords** Observational entropy, Block-coherence measures, Quantum resource degradation, Resource purity, Variational quantum algorithms

#### 1 Introduction

Quantum resource theory is a cornerstone of modern quantum information science. It provides a systematic framework for understanding quantum advantage by distinguishing between free states and resource states, as well as free operations and resource operations [1–6]. Within this paradigm, resource measures are typically scalar functions satisfying monotonicity—they do not increase under free operations. This ensures theoretical self-consistency. However, it also imposes a fundamental limitation: scalar measures cannot capture the quality changes of resource

Xiang Zhou\*1,2

during evolution. When we focus solely on the "quantity" of resources, the degradation process of resource "quality" remains hidden

To address this limitation, we propose a quantum resource degradation theory. We show that under free operations, valuable quantum resources are not merely consumed but rather transformed in form. Specifically, useful quantum coherence degrades into classical noise. This degradation process is often invisible to traditional scalar measures. However, it significantly affects the performance of quantum technologies.

Our framework builds on the decomposition of observational entropy (OE) [7–18]. OE generalizes Boltzmann entropy to the quantum realm. It describes the measurement uncertainty under coarse-grained measurements. For any initial state  $\rho$  and a given coarse-graining  $\mathcal{C} = \{\hat{P}_x\}$ , the coarse-graining process yields an ensemble  $\{\rho_x, p_x\}$ . Here,  $p_x = \text{Tr}[\hat{P}_x \rho \hat{P}_x]$  and  $\rho_x = \frac{\hat{P}_x \rho \hat{P}_x}{p_x}$ . Each state  $\rho_x$  belongs to a partitioned subspace  $\mathcal{H}_x$  with volume  $V_x = \text{Tr}[\hat{P}_x]$ .

<sup>(1)</sup>School of Mathematics and Computational Science, Shangrao Normal College, Shangrao 334001, People's Republic of China (2)Jiangxi Province Key Laboratory of Applied Optical Technology, School of Physical Science and Intelligent Education, Shangrao Normal University, Shangrao 334001, China E-mail: zhoux2032@163.com

2 Xiang Zhou\*<sup>1,2</sup>

Within each such subspace, we define  $\kappa_x = \frac{\hat{P}_x}{V_x}$  as the corresponding maximally mixed state. The relative entropy

$$D(\rho_x \mid\mid \kappa_x) = \text{Tr}[\rho_x(\log_2 \rho_x - \log_2 \kappa_x)]$$
  
= \log\_2 V\_x - S(\rho\_x), (1)

quantifies the deviation of  $\rho_x$  from  $\kappa_x$ . A larger value indicates that  $\rho_x$  is closer to a pure state; a smaller value indicates that it is closer to the maximally mixed state.

The difference

$$\mathcal{O}_{\mathcal{C}}(\rho) = S_{\mathcal{C}}(\rho) - S(\rho), \tag{2}$$

quantifies the misalignment between the system state and the measurement reference frame defined by the coarse-graining [16–18]. If OE equals the von Neumann entropy, the coarse-graining is consistent with the state; otherwise, an inconsistency exists. Hence, in this work, we refer to  $\mathcal{O}_{\mathcal{C}}$  as the total inconsistency.

Capturing this qualitative degradation requires moving beyond scalar measures and examining the internal structure of resource. To this end, we establish a theoretical framework based on the structural decomposition of the total resource. This decomposition reveals that there exists a dominant degradation pathway under free operations: the resource itself undergoes a transformation—quantum coherence is lost and converted into classical noise. This process can occur without a net change in the total resource quantity, explaining why performance may degrade even when traditional measures indicate that the total resource quantity is unchanged.

Optimization stagnation is a critical challenge in variational quantum algorithms (VQAs) [19, 20], where the optimization process halts despite continued parameter updates. Specifically, the cost function ceases to decrease and becomes trapped at a suboptimal value, exhibiting a pronounced plateau. This does not imply that the algorithm has terminated entirely; rather, the parameter updates become effectively undirected-akin to random walks on a flat landscape-with no consistent descent toward lower minima.

The main cause of stagnation is gradient vanishing: the gradients of the cost function with respect to the parameters approach zero. As a result, the optimizer loses the directional information needed to guide the search toward better solutions. Within our resource-theoretic framework, stagnation stems not from a quantitative reduction in resources, but from a qualitative degradation. Even when the total resource  $\mathcal{O}_{\mathcal{C}}$  remains approximately constant, the transformation of inter-block coherence  $\mathcal{C}_{\rm rel}$  into intrablock noise  $\mathcal{D}_{\rm rel}$  reduces the resource purity metric  $\eta$ . A decline in  $\eta$  signifies the dominance of classical noise over quantum coherence, which in turn induces gradient vanishing and leads to optimization stagnation. This provides a new interpretation of barren plateaus that goes beyond conventional entanglement-based explanations.

The structure of this paper is as follows: Section 2 reviews essential background knowledge; Section 3 presents the decomposition framework and degradation theory; Section 4 compares our approach with existing resource

theories; Section 5 applies the theory to VQAs; Section 6 concludes with a discussion of implications and future directions.

#### 2 Background Knowledge

This section reviews the essential background knowledge required to understand the theory presented in this work. Section 2.1 introduces OE, followed by the framework of  $\mathcal{C}_{\rm rel}$  in Section 2.2.

#### 2.1 Observational Entropy

For a coarse-graining  $C = {\hat{P}_x}$  and an initial state  $\rho$ , OE is defined as [7,17]

$$S_{\mathcal{C}}(\rho) = -\sum_{x} p_x \log_2 \frac{p_x}{V_x},\tag{3}$$

where  $p_x = \text{Tr}[\hat{P}_x \rho \hat{P}_x]$  and  $V_x = \text{Tr}(\hat{P}_x)$ .

In [16–18], the difference from von Neumann entropy is:

$$\mathcal{O}_{\mathcal{C}}(\rho) = S_{\mathcal{C}}(\rho) - S(\rho). \tag{4}$$

This difference measures the extent of superposition in mixed states relative to an orthogonal decomposition of the Hilbert space [16]. It satisfies:

(C1)  $\mathcal{O}_{\mathcal{C}}(\rho) \geq 0$ 

(C2)  $\mathcal{O}_{\mathcal{C}}(\rho) = 0$  if and only if  $\rho = \sum_{x} \frac{p_x}{V_x} \hat{P}_x$ 

(C3)  $\mathcal{O}_{\mathcal{C}}(U\rho U^{\dagger}) = \mathcal{O}_{\mathcal{C}}(\rho)$  for  $U = \bigoplus_{j} U_{j}$  commuting with  $\mathcal{C}$ 

(C4)  $\mathcal{O}_{\mathcal{C}}(\rho)$  is convex

#### 2.2 Resource Theory of Inter-block Coherence

The resource theory of block coherence, originally proposed by Åberg [1], extends coherence to projective measurements. Let  $\mathcal{H} = \bigoplus_x \mathcal{H}_x$  be a direct sum of orthogonal subspaces  $\mathcal{H}_x$  with projectors  $\hat{P}_x$ . The set of Block-incoherent (BI) states is

$$\mathcal{I}_{\mathrm{B}}(\mathcal{H}) = \left\{ \sum_{x} \hat{P}_{x} \sigma \hat{P}_{x} \mid \sigma \in \mathcal{S} \right\}. \tag{5}$$

The block-dephasing operation is defined as

$$\Delta[\sigma] = \sum_{x} \hat{P}_{x} \sigma \hat{P}_{x}. \tag{6}$$

Maximally Block-Incoherent (MBI) operations  $\Lambda_{\rm MBI}$  are quantum channels satisfying [21–25]

$$\Lambda_{\mathrm{MBI}}[\mathcal{I}_{\mathrm{B}}(\mathcal{H})] \subseteq \mathcal{I}_{\mathrm{B}}(\mathcal{H}). \tag{7}$$

A canonical measure of block coherence is the relative entropy:

$$C_{\rm rel}(\rho, \mathcal{C}) = S(\Delta[\rho]) - S(\rho). \tag{8}$$

It satisfies the following:

- (B1) Faithfulness:  $C_{\rm rel}(\rho, \mathcal{C}) \geq 0$  with equality iff  $\rho = \rho_{BI}$ .
- (B2) Monotonicity:  $C_{\rm rel}(\Lambda_{\rm MBI}[\rho], C) \leq C_{\rm rel}(\rho, C)$  for any MBI map.

(B3) Convexity: 
$$C_{\text{rel}}(\sum_x p_x \rho_x, C) \leq \sum_x p_x C_{\text{rel}}(\rho_x, C)$$
.

Physically,  $C_{\rm rel}$  quantifies the additional uncertainty arising from inter-block coherence. If the system possesses no coherence between blocks, that is, if it is already block-diagonal, then  $C_{\rm rel}(\rho,\mathcal{C})=0$ . If the system possesses  $C_{\rm rel}$ , then  $\Delta[\rho]$  is more disordered than  $\rho$ . This occurs because the dephasing operation eliminates coherence, thereby converting quantum superposition into classical probability and increasing the entropy. Finally, the convexity of  $C_{\rm rel}$  implies that mixing quantum states cannot create additional resources. Consequently, the resulting resource measure cannot exceed the average of the resources present in the constituent states. This is consistent with the physical intuition that stochastic mixing—a free and often resource-destroying operation—should average out or diminish resources rather than create them.

#### 3 Quantum Resource Degradation Theory

Building on the foundations of OE and block coherence introduced in Section 2, we now present the decomposition framework that underlies our theory.

#### 3.1 OE Decomposition

This section formally introduces the decomposition framework of OE.

For a coarse-graining  $C = {\hat{P}_x}$  and state  $\rho$ , we have [11]

$$S_{\mathcal{C}}(\rho) = S\left[\sum_{x} \hat{P}_{x} \rho \hat{P}_{x}\right] + \sum_{x} p_{x} D[\rho_{x} \mid\mid \kappa_{x}], \tag{9}$$

where  $\rho_x = \frac{\hat{P}_x \rho \hat{P}_x}{p_x}$  and  $\kappa_x = \frac{\hat{P}_x}{V_x}$ . The core relationship is given by:

$$\mathcal{O}_{\mathcal{C}}(\rho) = \mathcal{C}_{\text{rel}}(\rho, \mathcal{C}) + \mathcal{D}_{\text{rel}}(\rho), \tag{10}$$

where  $\mathcal{D}_{\mathrm{rel}}(\rho) = \sum_x p_x D[\rho_x \mid \mid \kappa_x]$  is the intra-block noise. Although Equation 10 represents a mathematical identity, its physical significance lies in structurally separating the total resource into two physically distinct components. This decomposition reveals that  $\mathcal{O}_{\mathcal{C}}$  comprises inter-block coherence ( $\mathcal{C}_{\mathrm{rel}}$ ) and intra-block noise ( $\mathcal{D}_{\mathrm{rel}}$ ). This allows us to track how resource quality degrades under free operations, even when the total quantity is conserved.

The framework identifies a key degradation pathway where quantum coherence transforms into classical noise. This conversion can occur while approximately conserving  $\mathcal{O}_{\mathcal{C}}$ , explaining performance decline even when traditional measures indicate constant resource quantity.

 $\mathcal{O}_{\mathcal{C}}$  is not a standard coherence measure in traditional resource theories, but it serves as a measure of total inconsistency between the quantum state and the classical

reference frame defined by the coarse-graining. This framework extends beyond conventional coherence measures by capturing both quantum and classical aspects of resource degradation.

This structural approach addresses a fundamental limitation of conventional resource theories: the inability to track resource quality changes under free operations. It provides new insights into quantum resource degradation, particularly in variational algorithms where resource quality determines performance.

#### 3.2 Resource Purity

Building on the decomposition of OE, we further introduce the definition of  $\eta$ .

**Definition 1** (Resource Purity) For a coarse-graining  $C = \{\hat{P}_x\}$  and an initial state  $\rho$ , resource purity is defined as:

$$\eta(\rho) := \frac{\mathcal{C}_{\text{rel}}(\rho, \mathcal{C})}{\mathcal{O}_{\mathcal{C}}(\rho)},\tag{11}$$

when  $\mathcal{O}_{\mathcal{C}}(\rho) = 0$ , we define  $\eta(\rho) = 0$ , as the state is fully consistent with the coarse-graining.

The resource purity  $\eta$  is derived from the decomposition in Equation 10. It quantifies the proportion of valuable quantum coherence in the total inconsistency, providing a quality-aware metric that traditional scalar measures lack.

- Physical Meaning: A high value of  $\eta$  indicates high resource quality, whereas a low value signifies that the resource is dominated by intra-block noise.
- Numerical Example: Suppose  $\mathcal{O}_{\mathcal{C}}(\rho) = 0.8$ , where  $\mathcal{C}_{\rm rel}(\rho,\mathcal{C}) = 0.6$  and  $\mathcal{D}_{\rm rel}(\rho) = 0.2$ . Then,  $\eta(\rho) = \frac{0.6}{0.8} = 0.75$ . This indicates that 75% of the state's total inconsistency consists of useful quantum coherence, signifying high resource quality. If, after some operation,  $\eta$  decreases to 0.4, it indicates a significant degradation in resource quality.

The definition of  $\eta$  is motivated by a one-way implication: if  $\mathcal{O}_{\mathcal{C}}(\rho) = 0$ , then  $\mathcal{C}_{\mathrm{rel}}(\rho, \mathcal{C}) = 0$ , but the reverse is not true [16]. A higher ratio means that more of the  $\mathcal{O}_{\mathcal{C}}$  comes from the valuable resource, signifying a higher quality resource state. Conversely, a lower ratio indicates a lower-quality resource, saturated with excessive intrablock noise. This establishes a quality-aware criterion for comparing resource states and optimizing distillation protocols.

To assess its effectiveness and limitations as an auxiliary diagnostic tool, we now rigorously examine its mathematical properties.

- 1. Normalization:  $0 \le \eta(\rho) \le 1$ . Specifically,  $C_{\rm rel}(\rho, C) = 0$  implies  $\eta(\rho) = 0$ , and  $D_{\rm rel}(\rho) = 0$  implies  $\eta(\rho) = 1$ .
- 2. Monotonicity:  $\eta(\Lambda(\rho)) \leq \eta(\rho)$  for any free operation  $\Lambda$ .

#### 3.3 Nonconvexity of $\mathcal{O}_{\mathcal{C}}$

The measure  $\mathcal{O}_{\mathcal{C}}$ , used throughout this work, is generally nonconvex. This property raises a question: does nonconvexity undermine its theoretical foundation as a resource measure?

We argue the opposite: such nonconvexity reflects physical phenomena that the traditional resource theory framework fails to capture. The conventional requirement of convexity stems from the implicit assumption that mixing states via free operations cannot create resources. In contrast,  $\mathcal{O}_{\mathcal{C}}$  measures the mismatch between the system state  $\rho$  and a classical perspective defined by the coarsegraining  $\mathcal{C}$ . This mismatch comprises two components:  $\mathcal{C}_{\rm rel}$  (a traditional resource) and  $\mathcal{D}_{\rm rel}$  (a non-traditional one).

The nonconvexity of  $\mathcal{O}_{\mathcal{C}}$  arises because mixing quantum states can increase the mismatch between the system state and the classical reference frame, and this has important physical implications:

- Physical Significance: The nonconvexity reflects the fundamental quantum principle that coherent superpositions cannot be created by classical mixing alone. An increase in  $\mathcal{O}_{\mathcal{C}}$  under mixing indicates the genuine generation of quantum resources.
- Compatibility with Resource Theory: While  $\mathcal{O}_{\mathcal{C}}$  itself is nonconvex, the valuable resource component,  $\mathcal{C}_{\mathrm{rel}}$ , satisfies all standard resource theory axioms (faithfulness, monotonicity, convexity). Thus, our framework bridges traditional convex resource theories with more general quantum characterizations.
- Theoretical Advantage: The nonconvex nature allows  $\mathcal{O}_{\mathcal{C}}$  to capture resource transformations that convex measures would miss. This includes the degradation pathway where coherence converts to noise without a net change in the total value.

This nonconvexity is essential, as it enables our theory to describe subtle degradation processes in practical quantum systems.

#### 3.4 Degradation Channels

Our goal is to demonstrate how resource quality declines through coherence-to-purity conversion when total resources are only approximately conserved. For this purpose, we construct specific degradation channels. We validate this mechanism through rigorous mathematical proofs and numerical examples, and we discuss the physical realization of these channels in real quantum systems.

The following definition outlines the transformation of resources under free operations and establishes the mathematical basis for constructing degradation channels.

**Definition 2** (Resource Transformation Pathway) For a coarse-graining  $C = \{\hat{P}_x\}$  and an initial state  $\rho$ . Under a free operation  $\Lambda$ , the transformation pathway of resource

is described by the following series of equations:

$$\Delta C_{\rm rel} = C_{\rm rel}(\Lambda(\rho), C) - C_{\rm rel}(\rho, C) \leq 0, 
\Delta D_{\rm rel} = D_{\rm rel}(\Lambda(\rho)) - D_{\rm rel}(\rho), 
\Delta O_{C} = O_{C}(\Lambda(\rho)) - O_{C}(\rho) = \Delta C_{\rm rel} + \Delta D_{\rm rel},$$
(12)

where  $|\Delta C_{\rm rel}|$  represents the magnitude of decrease in  $C_{\rm rel}$ , and  $|\Delta D_{\rm rel}|$  represents the change of  $D_{\rm rel}$ .

This paper focuses on scenarios in which, under specific free operations,  $C_{\rm rel}$  decreases ( $\Delta C_{\rm rel} < 0$ ) while  $D_{\rm rel}$  increases ( $\Delta D_{\rm rel} > 0$ ).

Based on this transformation pathway, we define degradation channels as free operations that systematically reduce  $\eta$ .

**Definition 3** (Degradation Channels): A degradation channel  $\Lambda$  is a free operation that systematically converts useful quantum coherence into classical noise, while approximately conserving the total resource quantity. We construct a specific degradation channel as follows:

$$\Lambda_{\alpha,\beta}(\rho) = (1 - \alpha)\rho + \alpha \mathcal{D}_{\beta}(\rho), \tag{13}$$

where  $\mathcal{D}_{\beta}(\rho) = \beta \Delta[\rho] + (1-\beta) \sum_{x} \hat{P}_{x} |\psi_{0}\rangle \langle \psi_{0}| \hat{P}_{x}$ . The parameter  $\alpha$  controls the overall noise level of the channel. The parameter  $\beta$  controls the relative weight between the two noise mechanisms in the degradation channels, reflecting the specific pathway of quantum resource transformation from coherence to noise.

#### - Why is this a free operation?

- $-\Delta[\rho]$ : This block-dephasing operation removes all inter-blocks and is a standard free operation.
- $-\sum_x \hat{P}_x |\psi_0\rangle\langle\psi_0|\hat{P}_x$ : This operation projects the target ground state onto various blocks, resulting in a block-diagonal state. Such state preparation is a free operation.
- $-\mathcal{D}_{\beta}(\rho)$ : This composite degradation operation combines the two noise mechanisms mentioned above.
- $-\Lambda_{\alpha,\beta}(\rho)$ : This is a convex combination of the identity, a dephased state, and a projected state. Since the set of free states is closed under convex combination and the dephasing operation is free, the overall channel maps free states to free states, thus qualifying as a free operation.
- Experimental Purpose: This channel enables the controlled simulation of resource degradation, facilitating the systematic observation of how  $\eta$  evolves during VQA optimization and how noise accumulates.

The definition of degradation channels leads to the following corollary.

**Corollary 1** *Under*  $\Lambda$ , the change of  $\eta$  is:

$$\eta(\Lambda(\rho)) \approx \eta(\rho) - \frac{|\Delta C_{rel}|}{\mathcal{O}_{C}(\rho)},$$
(14)

where the ratio  $\frac{|\Delta C_{rel}|}{\mathcal{O}_{\mathcal{C}}(\rho)}$  quantifies the relative loss of coherence with respect to the total inconsistency.

If  $\mathcal{O}_{\mathcal{C}}(\rho) = 0$ , then  $|\Delta \mathcal{C}_{\mathrm{rel}}| = \eta(\rho) = 0$  and consequently  $\eta(\Lambda(\rho)) = 0$ . The value of  $\eta$  remains approximately invariant under degradation channels if and only if the change in  $\mathcal{O}_{\mathcal{C}}$ ,  $\Delta \mathcal{O}_{\mathcal{C}}$ , is negligible.

Let  $\Delta \eta = \eta(\rho) - \eta(\Lambda(\rho))$ . This quantity,  $\Delta \eta$ , reflects the degradation of resource quality induced by the channel. We classify resource degradation into three levels based on the value of  $\Delta \eta$ :

- Minor degradation ( $\Delta \eta \in (0, 0.2)$ ): The decline in resource quality may be due to slight noise or optimization stagnation.
- Significant degradation ( $\Delta \eta \in [0.2, 0.4)$ ): A noticeable decline in resource quality, which may substantially impact the ongoing quantum task, such as algorithm performance.
- Severe degradation ( $\Delta \eta \geq 0.4$ ): Serious deterioration in resource quality, often accompanied by a BPP.

These thresholds for  $\Delta\eta$  can be adjusted for systems of different sizes.

The following theorem, which constitutes the core finding of our theory, demonstrates the transformation mechanism of resources under specific free operations.

**Theorem 1** (Resource Degradation Mechanism) There exists a degradation channel  $\Lambda$  and quantum states  $\rho$  such that:

- 1.  $C_{rel}$  decreases:  $\Delta C_{rel} < 0$ ,
- 2.  $\mathcal{D}_{rel}$  increases:  $\Delta \mathcal{D}_{rel} > 0$ ,
- 3.  $\mathcal{O}_{\mathcal{C}}$  remains approximately conserved:  $|\Delta \mathcal{D}_{rel}| \approx |\Delta \mathcal{C}_{rel}|$ .

Under these conditions,  $\Delta \mathcal{O}_{\mathcal{C}} \approx 0$ . This indicates that while the total uncertainty remains approximately constant, the resource quality undergoes significant degradation.

This theorem captures the essence of degradation: although the total resource quantity remains unchanged, the intrinsic resource quality deteriorates. This occurs through the conversion of quantum coherence into classical noise.

The evolution of the relevant physical quantities in the proof of Theorem 1 (see Appendix 6) is shown in Figure 1. When  $\varepsilon$  approaches 1, the quantum state undergoes near-complete collapse toward the  $|00\rangle\langle00|$ . This extreme regime exhibits several distinctive characteristics that deviate from our theoretical focus. Theorem 1 provides an existence proof for degradation channels that produce the coherence-to-noise transformation. The theorem does not require examining the entire parameter space; it suffices to show that such channels operate effectively within specific regions. The critical degradation mechanism is fully captured within  $\varepsilon \in [0, 0.26]$ , rendering an extension to higher values unnecessary for validating our theoretical claims. The observed transformation between coherence and purity within this region provides compelling evidence for the existence of degradation channels described in Theorem 1. Therefore, we restrict  $\varepsilon$  to the interval [0, 0.5].

Subplot (a) of Figure 1 shows the evolution of resource components as a function of  $\varepsilon$ .  $\mathcal{O}_{\mathcal{C}}$  exhibits a convex profile for  $\varepsilon$  in [0, 0.26], while  $\eta$  declines. This convexity indicates a non-monotonic degradation process. The convex

shape of  $\mathcal{O}_{\mathcal{C}}$  demonstrates that the resource transformation is not linear. The initial decrease corresponds to a temporary reduction in total inconsistency, while the subsequent recovery indicates compensatory effects between the competing components. Despite this variation, the conservation of  $\mathcal{O}_{\mathcal{C}}$  at the region's endpoint confirms the theoretical prediction of approximate total resource conservation. Concurrently,  $\eta$  undergoes significant degradation throughout this region. The purity metric drops from approximately 0.58 to 0.29, representing a change exceeding 0.2. According to the classification criteria established in the paper, this magnitude of purity reduction qualifies as significant degradation.

Subplot (b) of Figure 1 displays the differential changes of resource measures.  $C_{\rm rel}$  shows negative values, confirming coherence consumption.  $\mathcal{D}_{\rm rel}$  exhibits positive values, indicating purity generation.  $\mathcal{O}_{\mathcal{C}}$  remains near zero within the degradation region, validating total resource conservation during the transformation process.

Subplot (c) of Figure 1 quantifies the conversion rate between  $C_{\rm rel}$  and  $D_{\rm rel}$ . The efficiency  $\frac{\Delta D_{\rm rel}}{|C_{\rm rel}|}$  approaches 1 in specific regions, indicating ideal transformation, i.e., each unit of lost quantum coherence converts precisely into one unit of gained classical purity. This confirms the theoretical prediction that quantum coherence converts precisely into classical noise under optimal conditions.

Subplot (d) of Figure 1 validates the three conditions of Theorem 1 at the critical point. It demonstrates  $\Delta C_{\rm rel} < 0$ ,  $\Delta \mathcal{D}_{\rm rel} > 0$  and  $\Delta \mathcal{O}_{\mathcal{C}} \approx 0$  simultaneously. The significant drop in  $\eta$  confirms resource quality degradation while total resources remain conserved.

#### 3.5 Results and Discussion

Our framework provides a new diagnostic perspective for quantum optimization challenges. Unlike traditional explanations that focus primarily on entanglement saturation or randomness, our theory emphasizes resource quality degradation as a fundamental mechanism underlying optimization failures. The resource purity metric  $\eta$  offers distinctive diagnostic capabilities:

#### Theoretical Diagnostic Framework:

Early Warning Capability: A decline in  $\eta$  often precedes visible optimization stagnation, serving as an early indicator of resource quality degradation.

Failure Mode Discrimination:  $\eta$  distinguishes between optimization failures due to insufficient resource quantity (low  $\mathcal{O}_{\mathcal{C}}$ ) versus degraded resource quality (low  $\eta$  despite adequate  $\mathcal{O}_{\mathcal{C}}$ ).

**Degradation Pathway Identification:** The transformation of coherence-to-noise  $(C_{\rm rel} \to \mathcal{D}_{\rm rel})$  provides a specific mechanistic explanation for performance deterioration

In Section 5, we validate this framework through application to the BPP in VQAs, demonstrating how real-time monitoring of  $\eta$  can diagnose and potentially mitigate optimization stagnation.

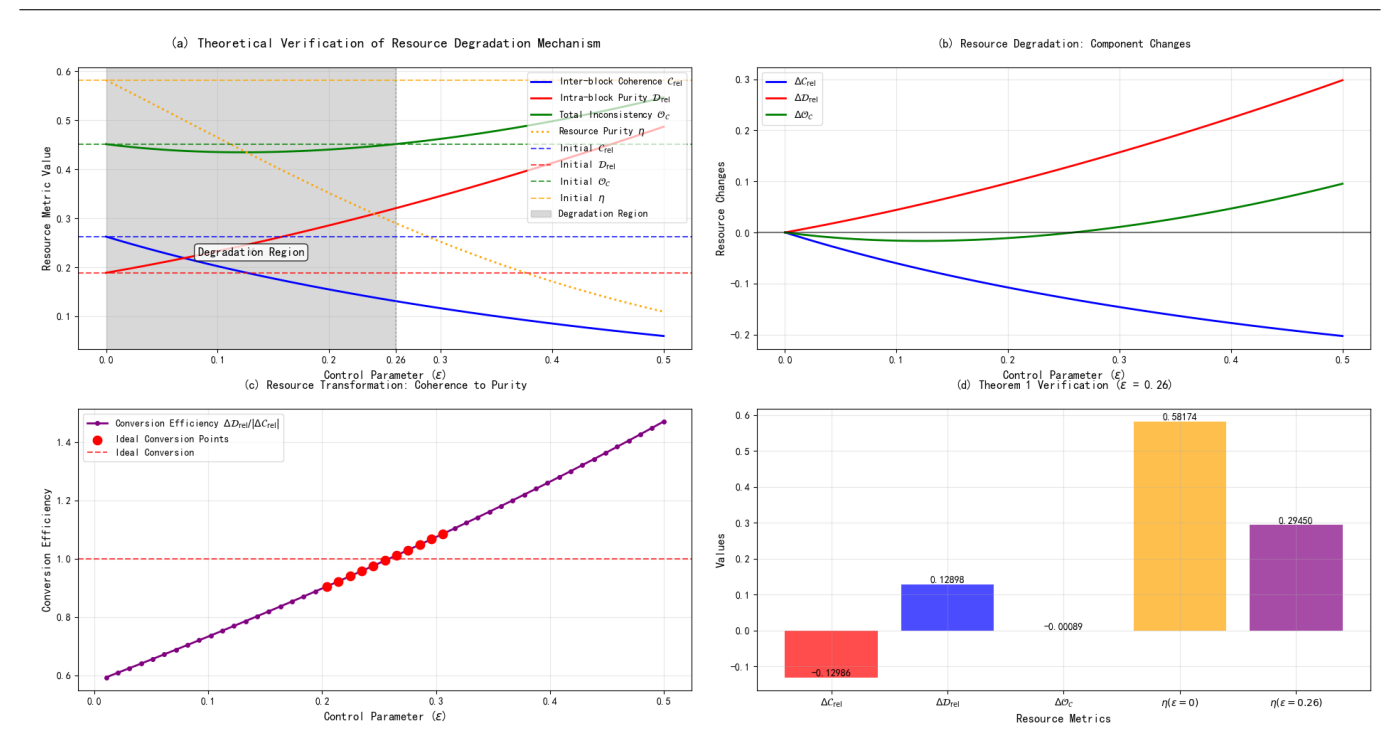


Figure 1: Evolution of quantum resource metrics versus the control parameter  $\varepsilon$ . In Subplots (a) and (b), the blue curves represent  $\mathcal{C}_{\rm rel}$  and  $\Delta \mathcal{C}_{\rm rel}$ ; the red curves represent  $\mathcal{D}_{\rm rel}$  and  $\Delta \mathcal{D}_{\rm rel}$ ; the green curves represent  $\mathcal{O}_{\mathcal{C}}$  and  $\Delta \mathcal{O}_{\mathcal{C}}$ ; the orange curve represents  $\eta$ . Subplot (a) shows the evolution of quantum resource components versus the control parameter  $\varepsilon$ . Subplot (b) displays the differential changes of resource measures. Subplot (c) quantifies the conversion rate between  $\mathcal{C}_{\rm rel}$  and  $\mathcal{D}_{\rm rel}$ . Subplot (d) validates the three conditions of Theorem 1 at the critical point. Let  $\varepsilon$  being [0,0.5].

To better elucidate the innovations and unique features of the proposed theory, we now provide a systematic comparison with existing resource-theoretic frameworks.

#### 4 Comparison with Existing Resource Theories

This section places our theory within the broader landscape of quantum resource theories. By clarifying the common foundations and distinctive features of our approach, we aim to highlight its theoretical novelty and practical utility.

#### 4.1 Contrast with Traditional Scalar Resource Theories

Conventional quantum resource theories establish a powerful paradigm for quantifying quantum advantage through the following elements:

- Free states  $(\mathcal{F})$ : States that are easily preparable within constraints.
- Free operations ( $\Lambda_{\text{free}}$ ): Operations that cannot create resources from free states.
- Resource measures  $(M(\rho))$ : Scalar functions satisfying monotonicity:  $M(\Lambda_{\text{free}}(\rho)) \leq M(\rho)$ .

Our framework adheres to this paradigm: the free states are the block-incoherent (BI) states, the free operations include the degradation channels that we construct, and the  $\mathcal{O}_{\mathcal{C}}$  serves as a foundational resource measure.

– Free states: BI states  $\rho_{\text{BI}} = \sum_{x} \frac{p_x}{V_x} \hat{P}_x$ .

- Free operations: Degradation channels  $\Lambda$ .
- Resource measures: Total inconsistency  $\mathcal{O}_{\mathcal{C}}$ .

The conceptual advance of our theory is highlighted by contrasting it with traditional scalar resource theories in Table 1.

Table 1 highlights a fundamental shift in perspective. Traditional theories focus on the consumption of total resources ( $\Delta M \leq 0$ ). Our theory, through the decomposition of OE, reveals the transformation between the two components of  $\mathcal{O}_{\mathcal{C}}$ :  $\mathcal{C}_{\mathrm{rel}}$  and  $\mathcal{D}_{\mathrm{rel}}$ .

Consequently, when  $\Delta M \approx 0$ , traditional theories can only indicate that resources are not consumed, offering limited explanatory power. In contrast, our theory explains scenarios where performance degrades despite apparent resource conservation. The degradation occurs through the transformation of  $\mathcal{C}_{\rm rel}$  into  $\mathcal{D}_{\rm rel}$ , which decreases  $\eta$ . This provides a new physical explanation for performance degradation in the absence of a significant decrease in total resources.

This distinction is crucial for explaining phenomena like the barren plateau, where algorithm performance deteriorates even when total resources are conserved.

#### 4.2 Connection with Purity and Mixedness Measures

Conventional purity is typically measured by  $\text{Tr}(\rho^2)$  or von Neumann entropy  $S(\rho) = -\text{Tr}(\rho \log \rho)$ . These are global measures describing the state's deviation from the maximally mixed state. Decoherence typically increases the mixedness of a system (i.e., decreases its purity).

Aspect	Traditional Theory	Our Theory
Primary Focus	Resource quantity $M(\rho)$	Resource composition: $C_{\rm rel}$ vs $D_{\rm rel}$
Resource Evolution	Consumption: $\Delta M \leq 0$	Transformation: $\mathcal{C}_{\mathrm{rel}} \to \mathcal{D}_{\mathrm{rel}}$
Diagnostic Power	Limited when $\Delta M \approx 0$	Explains performance degradation even when $\Delta \mathcal{O}_{\mathcal{C}} \approx \text{constant}$
Quality Assessment	Not available	$\eta$ quantifies quality
Barren Plateaus Explanation	Excessive entanglement or randomness	Resource quality degradation

Table 1: Comparison between Traditional Resource Theory and Our Theory

In our theory,  $\mathcal{D}_{\rm rel}$  measures the intra-block noise within subspaces, while  $\eta$  represents resource quality. Our theory indicates that during resource degradation,  $\mathcal{D}_{\rm rel}$  increases while  $\eta$  decreases. This appears to contradict the intuition that noise leads to mixing.

The seemingly contradictory behavior—where noise increases  $\mathcal{D}_{\rm rel}$  while typically decreasing global purity—arises from their different reference frames, which are defined by the coarse-graining. This critical distinction is systematically summarized in Table 2.

The resolution highlights the nuanced perspective of our theory. Free operations (such as block dephasing  $\Delta$ ) destroy  $C_{\rm rel}$ , making the system more mixed globally (i.e., increasing  $S(\rho)$ ). However, within each coarse-grained subspace, such operations may push the state toward a more deterministic distribution, thereby increasing its local predictability.

Consider a practical example: a quantum state undergoing dephasing noise:

- Global perspective: Coherence between blocks is destroyed → increased mixedness → decreased global purity.
- Local perspective: Within each block, the state may become more deterministic  $\rightarrow$  increased local predictability  $\rightarrow$  increased  $\mathcal{D}_{rel}$ .

Measure	Reference Frames	Physical Interpretation
${ m Tr}( ho^2)$	Entire Hilbert space $\mathcal{H}$	Overall mixedness
$\mathcal{D}_{ extbf{rel}}( ho)$	Individual subspaces $\mathcal{H}_x$	intra-block noise

Table 2: Comparison between global purity  $\text{Tr}(\rho^2)$  and intrablock noise  $\mathcal{D}_{\text{rel}}(\rho)$ 

Therefore,  $\mathcal{D}_{\rm rel}$  measures the deviation from the maximally mixed state within each subspace. It captures a form of local noise that is structured within the subspaces, rather than global randomness. Resource degradation precisely represents the transformation from valuable non-local coherence to less useful intra-block noise.

4.3 Comparison with Traditional Entanglement Measures

The advantage of our metric  $\eta$  over traditional resource measures is demonstrated by comparing it with entanglement entropy.

As shown in Table 3, while entanglement entropy effectively detects resource consumption, it fails to distinguish between the conversion of coherence into noise and a mere reduction in resources. In contrast,  $\eta$  specifically captures resource quality degradation, offering a more refined diagnosis for optimization problems such as the BPP.

#### 4.4 Summary of Theoretical Positioning

The preceding comparisons establish the unique contribution of our theory. Rather than supplanting existing resource theories, our framework integrates and extends them by introducing a structural perspective on resource composition. The core advancement is a paradigm shift from quantifying the amount of resources to characterizing their form.

This is achieved by combining the concepts of coherence and intra-block noise into a single overarching measure,  $\mathcal{O}_{\mathcal{C}}$ , and then exposing the trade-off between its components under free operations. This unification allows our theory to:

Explain performance degradation in scenarios where traditional scalar measures indicate resource conservation, thereby addressing a key limitation in understanding the barren plateau.

Provide a quality-aware diagnostic tool  $(\eta)$  that offers early warnings and mechanistic insights beyond what is possible with measures of entanglement or global mixedness.

In conclusion, this work establishes resource quality management as a complementary paradigm to traditional resource quantification, providing a more nuanced and powerful framework for diagnosing and optimizing quantum technologies.

#### 5 Resource Degradation Theory in VQAs

We now apply our theory to VQAs. We demonstrate how the metric  $\eta$  serves as a diagnostic tool to provide a new perspective on optimization stagnation, particularly

Aspect	Entanglement Entropy	Resource Purity $\eta$
Diagnostic Capability	Detects resource consumption	Detects resource quality degradation
Barren Plateau Insight	Indicates entanglement saturation	Reveals coherence-to-noise transformation
Response to Noise	Decreases under decoherence	Specifically tracks quality transformation
Guidance for Optimization	Limited for quality assessment	Directs toward high-quality resource regions

Table 3: Comparison between Entanglement Entropy and  $\eta$ 

the BPP. Through controlled numerical experiments, we track the evolution of resource quality during optimization, thereby validating the predictions of our degradation framework.

#### 5.1 Experimental Setup

#### 5.1.1 System Model and Hamiltonian

We study a 4-qubit transverse-field Ising model with periodic boundary conditions  $Z_5 = Z_1$ , described by the Hamiltonian [26]:

$$H = -\sum_{i=1}^{4} Z_i Z_{i+1} - h \sum_{i=1}^{4} X_i.$$
 (15)

The transverse field strength is set to h=1, a standard choice that corresponds to the quantum critical point. We select this model for its clear energy level structure and well-studied entanglement properties. These features provide a physically meaningful basis for our coarse-graining scheme.

#### 5.1.2 Coarse-graining Scheme

In VQAs, the goal is to find the low-energy states of a problem Hamiltonian. Therefore, selecting the energy eigenbasis for coarse-graining is a natural choice.

$$\hat{P}_x = \sum_{i \in I_-} |E_i\rangle\langle E_i|,\tag{16}$$

where  $I_x$  represents the set of indices belonging to the energy subspace x, with  $x \in \{\text{low}, \text{medium}, \text{high}\}.$ 

The Hilbert space is partitioned into three energy subspaces:

- Low-energy subspace  $(E < E_{\min} + 0.3\Delta E)$ , where  $\Delta E = E_{\max} E_{\min}$ .
- Medium-energy subspace

$$E_{\min} + 0.3\Delta E \le E \le E_{\max} - 0.3\Delta E$$
,

- High-energy subspace  $(E > E_{\text{max}} - 0.3\Delta E)$ ,

#### 5.1.3 Cost Function

This subsection defines the cost function used for optimizing the VQA. The cost function is the expectation value of the system Hamiltonian with respect to the parameterized quantum state.

$$f(\vec{\theta}) = \langle \psi(\vec{\theta}) | H | \psi(\vec{\theta}) \rangle, \tag{17}$$

where  $|\psi(\vec{\theta})\rangle$  is the ansatz state prepared by the parameterized quantum circuit  $U(\vec{\theta})$ , and  $\vec{\theta}$  represents the tunable parameters of the circuit.

#### 5.1.4 Circuit Structure

We utilize a hardware-efficient ansatz [27,28], the detailed architecture of which is illustrated in Figure 3.

$$U(\vec{\theta}) = \left(\prod_{l=1}^{4} \mathcal{L}_l(\vec{\theta})\right) \left(\prod_{i=0}^{3} H_i\right),\tag{18}$$

where 
$$\mathcal{L}_{l}(\vec{\theta}) = \left(\prod_{i=0}^{3} R_{x}(\vec{\theta}_{l,i}^{x}) R_{y}(\vec{\theta}_{l,i}^{y})\right) \left(\prod_{i=0}^{3} CX_{i,i+1}\right)$$
 represents the *l*-th quantum circuit layer.

The circuit prepares the ansatz state  $|\psi(\vec{\theta})\rangle$  by applying an initial layer of Hadamard gates to all qubits, followed by L=4 identical layers. Each layer  $\mathcal{L}_l(\vec{\theta})$  consists of parameterized single-qubit rotations and a linear chain of CNOT gates for entanglement. This design, with a total of 32 tunable parameters, offers a balance between expressiveness and suitability for current and near-term noisy quantum devices. Its structure is well-suited for the systematic studying resource degradation.

#### 5.1.5 Optimization Protocol and Parameter Update Rules

This subsection details the three-phase degradation protocol and the parameter update rule used during the optimization process. This setup simulates the transition from an ideal optimization environment to one with strong degradation.

The degradation protocol defines how artificially introduced noise varies over time, simulating the accumulation of noise in real-world hardware that degrades VQA performance

It controls the intensity of the degradation channel  $\Lambda_{\alpha,\beta}$  (Equation 13) applied to the quantum state through

the degradation strength parameter  $\alpha$ . This channel systematically consumes valuable  $C_{rel}$  and converts it into  $\mathcal{D}_{\rm rel}$ , thereby directly lowering  $\eta$ .

#### - Degradation Protocol:

- Phase I (0-30): No degradation ( $\alpha = 0$ ). This phase simulates a noiseless optimization environment, where the algorithm can freely explore the Hilbert space to find the optimal solution. It establishes a performance baseline under ideal conditions.
- Phase II (30-60): Linear ramp-up of degradation ( $\alpha$  from 0.1 to 0.4). This phase simulates mild to moderate noise effects that begin to impede the optimization process, analogous to running a medium-depth circuit on a current and nearterm noisy quantum devices. device. In this phase, we observe how an initial decline in  $\eta$  affects the optimization progress (e.g., by slowing the descent of the cost function).
- **Phase III (60-150):** Strong degradation ( $\alpha$  from 0.4 to 0.8). This phase simulates the algorithm becoming trapped in a region of severe resource quality degradation where noise dominates and destroys the quantum coherence essential for computation. It demonstrates that even though optimization continues (parameters are still updated), the cost function cannot improve further due to the low quality of resources; that is, the algorithm has entered a barren plateau induced by resource degradation.

The parameter update rule describes how the classical optimizer adjusts the parameters  $\vec{\theta}$  of the quantum circuit based on the current step and cost function. This rule is designed to exhibit different behaviors across degradation phases, simulating the optimizer's response to varying noise levels.

#### - Parameter Update Rule:

$$\vec{\theta}^{(k+1)} = \vec{\theta}^{(k)} + \Delta \vec{\theta}^{(k)} \mod 2\pi. \tag{19}$$

- $-\Delta \vec{\theta}^{(k)}$  is the parameter update at step k, and its form varies with the phase.
  - The index k denotes the iteration step, serving as the temporal index for the entire process. It demarcates the different degradation phases and serves as the basis for the progress variable
- The variable p is a progress parameter, defined as  $p = \frac{k-30}{30}$  in the mild degradation phase and  $p = \frac{k-60}{90}$  in the strong degradation phase. - Early phase  $(k \le 30)$ :

$$\Delta \vec{\theta}^{(k)} = -0.05(0.1 \sin \vec{\theta}^{(k)} + \mathcal{N}(0, 0.05)). \tag{20}$$

In this noiseless environment, the update uses a stable learning rate (0.05). It consists of a weak gradient signal,  $0.1 \sin \vec{\theta}^{(k)}$  and a small stochastic exploration term,  $\mathcal{N}(0, 0.05)$ . This represents effective optimization under ideal conditions.

- The symbol  $\mathcal{N}(\mu, \sigma)$  denotes a random variable sampled from a Gaussian (normal) distribution with mean  $\mu$  and standard deviation  $\sigma$ . It represents stochastic fluctuations in the optimization process. During the early or mid phases, this noise helps the algorithm escape local minima. In the strong degradation phase, it models optimization steps that become almost entirely random due to the vanishing gradient signal caused by resource degradation.
- Mid phase  $(30 \le k \le 60)$ :

$$\Delta \vec{\theta}^{(k)} = -0.03 \sin \vec{\theta}^{(k)} (1 - 0.5p) + 0.2p \mathcal{N}(0, 0.5).$$
(21)

As the noise level  $\alpha$  increases, the learning rate is reduced (from 0.05 to 0.03). The weight of the gradient term decreases (governed by the progress factor p), while the amplitude of the random noise increases significantly. This simulates the optimizer struggling and relying more on randomness for direction.

- Strong degradation phase  $(k \ge 60)$ :

$$\Delta \vec{\theta}^{(k)} = -0.01 \sin \vec{\theta}^{(k)} (0.5 - 0.4p) + 0.5 \mathcal{N}(0, 1.0).$$
(22)

Under strong noise, the learning rate is minimal (0.01). The weight of the gradient term decreases from 0.5 to 0.1 as p increases, becoming almost negligible. Concurrently, the random noise term  $\mathcal{N}(0, 1.0)$  has a large amplitude and a high weight (0.5). Thus, the parameter updates become almost entirely random once the gradient signal vanishes a hallmark of the BPP.

In summary, the degradation protocol and parameter update rule are coupled. The protocol systematically lowers resource quality by controlling  $\alpha$ . The rule models the optimizer's response to this degradation. As  $\eta$  decreases, the effective gradient signal available to the optimizer weakens, and its behavior degenerates from directed gradient descent to undirected random walks.

This controlled experiment demonstrates how  $\eta$  precedes and causes optimization stagnation. This provides a novel diagnostic tool for the BPP.

#### 5.2 Resource Evolution under Degradation: Theoretical and Experimental Analysis

This section analyzes the evolution of quantum resource metrics under degradation channels, building on the experimental framework in Section 5.1. We monitor the dynamics of resource purity  $\eta$  and its components  $\mathcal{C}_{\mathrm{rel}}$  and  $\mathcal{D}_{\mathrm{rel}}$  to validate that resource quality degradation underlies VQA optimization stagnation.

Figure 2 presents comprehensive experimental validation of quantum resource degradation through four integrated analyses.

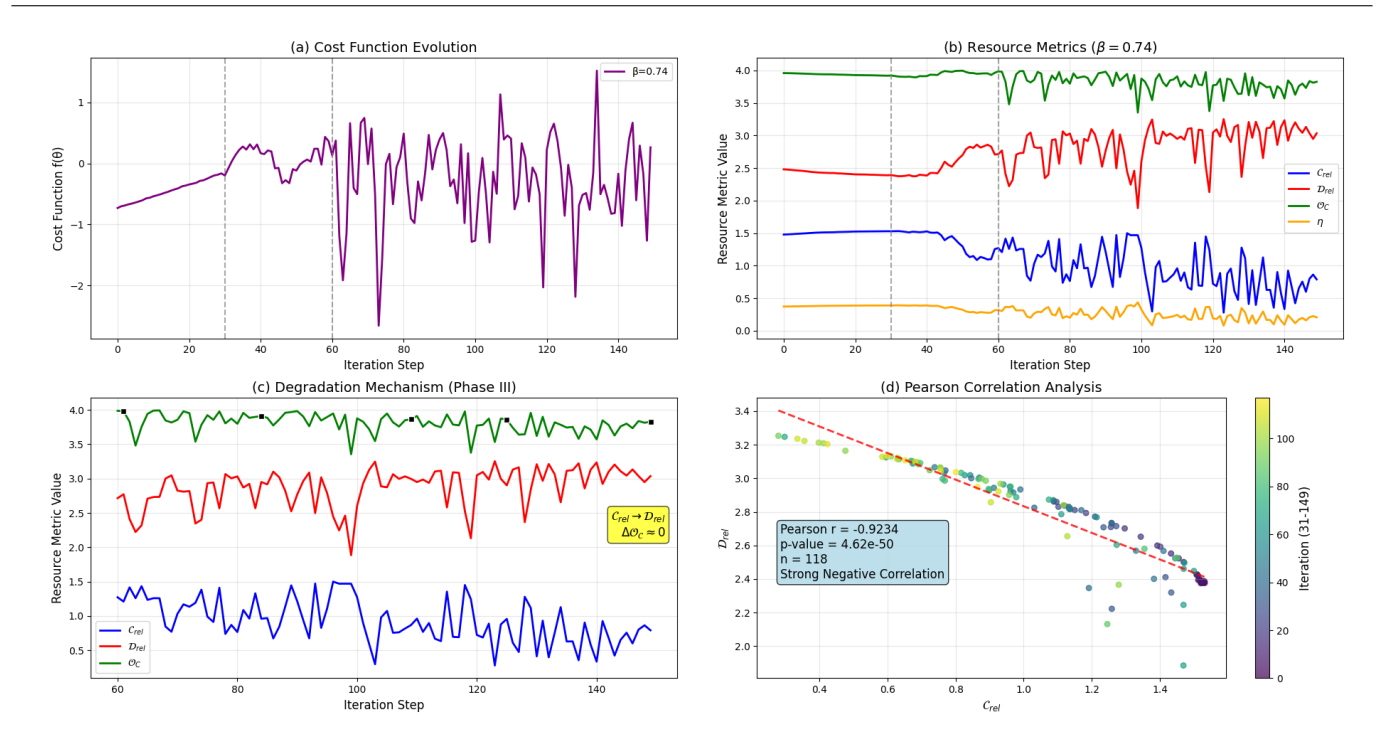


Figure 2: Verification of quantum resource degradation theory in VQAs. The figure consists of four Subplots: (a) shows the evolution of cost function , while (b) and (c) show the change of resource metrics for  $\beta=0.74$ . Subplot (d) shows the Pearson correlation analysis between  $\mathcal{C}_{\rm rel}$  and  $\mathcal{D}_{\rm rel}$ .

Subplot (a) of Figure 2 illustrates the cost function's progressive decline under the three-phase degradation protocol. During Phase I (iterations 0-30), optimization proceeds effectively without degradation. As degradation intensifies in Phase II (30-60), optimization progress slows substantially. Complete stagnation emerges in Phase III (60-150) despite continuous parameter updates, confirming that resource quality degradation directly induces barren plateau behavior.

Subplot (b) of Figure 2 reveals the fundamental transformation mechanism through resource metric evolution. Anti-phase oscillations between  $\mathcal{C}_{\mathrm{rel}}$  and  $\mathcal{D}_{\mathrm{rel}}$  demonstrate systematic conversion of quantum coherence into classical noise. Throughout this process,  $\mathcal{O}_{\mathcal{C}}$  remains approximately conserved, verifying structural resource transformation rather than quantitative depletion. The monotonic decline in  $\eta$  directly quantifies diminishing resource quality.

Subplot (c) of Figure 2 examines the strong degradation phase (iterations 60-150), where coherence-to-noise transformation becomes most pronounced. The persistent anti-correlation pattern confirms systematic conversion dynamics. Points where  $\Delta\mathcal{O}_{\mathcal{C}}\approx 0$  provide experimental validation of Theorem 1, demonstrating precise balance between quantum coherence consumption and classical noise generation under conserved total resources.

Subplot (d) of Figure 2 delivers rigorous statistical validation through Pearson correlation analysis.

The Pearson correlation coefficient r quantifies linear relationship between two variables, which is defined as:

$$r = \frac{\sum_{i=1}^{n} (x_i - \bar{x})(y_i - \bar{y})}{\sqrt{\sum_{i=1}^{n} (x_i - \bar{x})^2 \sum_{i=1}^{n} (y_i - \bar{y})^2}},$$
 (23)

where  $x_i$  and  $y_i$  represent  $\mathcal{C}_{\text{rel}}$  and  $\mathcal{D}_{\text{rel}}$  at iteration i, respectively.  $\bar{x}$  and  $\bar{y}$  represent the mean of  $\mathcal{C}_{\text{rel}}$  and  $\mathcal{D}_{\text{rel}}$ , respectively. n is the number of data points (iterations 31-149).

The Pearson correlation coefficient r and the p-value in Subplot (d) demonstrate a statistically significant inverse relationship. The coefficient r=-0.9309 quantifies the strong negative linear correlation between  $\mathcal{C}_{\rm rel}$  and  $\mathcal{D}_{\rm rel}$ , while the p-value ( $p\approx 0$ ) indicates extreme statistical significance. This p-value represents the probability of observing such a strong correlation by random chance under the null hypothesis of no relationship. The combination of r approaching -1 and p<0.001 provides compelling evidence against the null hypothesis, confirming that the observed anti-correlation is genuine and not due to random fluctuations. This statistical relationship validates the theoretical prediction of systematic conversion between coherence and noise components during resource degradation.

Collectively, these results establish quantum resource quality degradation as the fundamental mechanism driving algorithmic performance decline. The coherence-to-noise transformation explains optimization stagnation under conserved total resources, providing mechanistic insight into BPP beyond conventional explanations based solely on entanglement or randomness.

Figure 3 depicts the quantum circuit diagram corresponding to the hardware-efficient ansatz described in Section 5.1.4. This circuit generates the quantum states used to produce the resource evolution data shown in Figure 2. The final measurement stage maps each qubit to a dedicated classical register:  $q_0 \rightarrow c_0$ ,  $q_1 \rightarrow c_1$ ,  $q_2 \rightarrow c_2$ ,

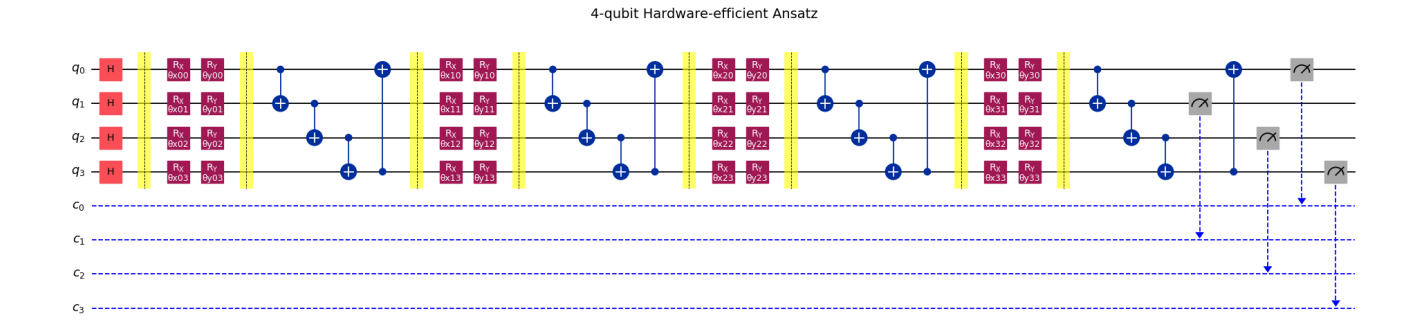


Figure 3: Circuit diagram of the 4-qubit hardware-efficient ansatz. The circuit includes an initial Hadamard layer, four parameterized layers with single-qubit rotations and CNOT gates, and a measurement stage. The final measurement stage enables classical processing and feedback for VQAs.

and  $q_3 \to c_3$ . This structured mapping facilitates classical processing and feedback within the VQA optimization loop. The circuit's design ensures consistent readout for computing resource metrics like  $\eta$ ,  $C_{\rm rel}$ , and  $\mathcal{D}_{\rm rel}$  analyzed in Figure 2.

#### 5.3 Resource Purity as a Diagnostic Tool

Our experiments show that the BPP arises from resource quality degradation. Traditional explanations focus on entanglement or randomness. Our theory emphasizes the coherence-to-noise transformation.

Key insights:

- Early Warning: A drop in  $\eta$  often precedes cost stagnation, signaling BPP early.
- Quality over Quantity: Failure can occur even with conserved total resources, highlighting quality's role.
- Mechanism: The anti-correlation between  $C_{rel}$  and  $D_{rel}$  confirms coherence converting to noise.

Proposed diagnostic protocol:

- Monitor  $\eta$  in real time during optimization.
- Act adaptively if  $\eta$  drops (e.g., switch optimizers, reset parameters).
- Use average  $\eta$  to evaluate ansatz designs, preferring high-quality resource architectures.

This approach explains BPP and guides robust VQA development. Numerical simulations validate  $\eta$  as a practical diagnostic. Tracking resource quality is crucial for noise-resilient algorithms and quantum advantage in the current and near-term noisy quantum devices era.

#### 6 Conclusion

This work establishes a quantum resource degradation theory based on the decomposition of OE. The theory reveals a fundamental degradation mechanism: under specific free operations, quantum coherence transforms into classical noise. This conversion conserves total resource quantity while critically diminishing resource quality.

Our framework overcomes key limitations of conventional resource theories. It provides structural insight into resource composition and evolution. The decomposition of  $\mathcal{O}_{\mathcal{C}}$  into  $\mathcal{C}_{\mathrm{rel}}$  and  $\mathcal{D}_{\mathrm{rel}}$  enables tracking of resource quality changes invisible to scalar measures.

Applied to VQAs, the theory reinterprets optimization stagnation as resource quality degradation rather than mere quantity reduction. The strong negative correlation between  $\mathcal{C}_{\rm rel}$  and  $\mathcal{D}_{\rm rel}$ , validated in Section 5.2, provides critical evidence for the coherence-to-noise transformation. This correlation confirms the systematic conversion mechanism underlying barren plateaus.

The resource purity metric  $\eta$  serves as both an explanatory tool and a practical diagnostic. It enables early detection of optimization stagnation and distinguishes failure modes. Monitoring  $\eta$  offers a pathway for developing mitigation strategies and noise-resilient algorithms.

This work introduces resource quality management as an essential complement to traditional quantification. It enhances optimization capabilities for current and nearterm noisy quantum devices.

Future research directions include: extending the theory to many-body systems and entangled resource scenarios; investigating universal conditions for degradation under general free operations; developing more robust quality 12 Xiang Zhou\*1,2

measures and efficient  $\eta$  estimation methods; implementing real-time  $\eta$  monitoring on noisy quantum hardware; designing adaptive optimization algorithms that preserve resource quality; and exploring connections with other quantum resource theories.

#### Acknowledgments

This research is supported by Jiangxi Province Key Laboratory of Applied Optical Technology [2024SSY03051].

#### Data availability

The datasets analysed during the current study are available from the corresponding author on reasonable request.

#### Appendix: Proof of Theorem 1

#### Proof. Step 1: System and Coarse-graining Setup

Consider a four-dimensional quantum system with Hilbert space  $\mathcal{H} = \mathbb{C}^4$  with the basis vectors  $|00\rangle$ ,  $|01\rangle$ ,  $|10\rangle$ ,  $|11\rangle$ . Define a coarse-graining  $\mathcal{C} = \{\hat{P}_1, \hat{P}_2\}$ , where:

$$\hat{P}_1 = |00\rangle\langle00| + |01\rangle\langle01|$$

$$\hat{P}_2 = |10\rangle\langle10| + |11\rangle\langle11|.$$
(24)

where subspace volumes are  $V_1=V_2=2$ , with corresponding maximally mixed states  $\kappa_1=\frac{1}{2}|00\rangle\langle00|+\frac{1}{2}|01\rangle\langle01|$  and  $\kappa_2=\frac{1}{2}|10\rangle\langle10|+\frac{1}{2}|11\rangle\langle11|$ .

#### Step 2: Initial State Construction

We construct the initial state  $\rho$  with specific properties to clearly demonstrate the resource degradation mechanism:

$$\begin{split} \rho = & \frac{3}{8} |00\rangle\langle00| + \frac{1}{4} |00\rangle\langle11| + \frac{1}{8} |01\rangle\langle01| \\ & + \frac{1}{8} |10\rangle\langle10| + \frac{1}{4} |11\rangle\langle00| + \frac{3}{8} |11\rangle\langle11|. \end{split} \tag{25}$$

This state is carefully chosen because:

- It possesses **significant**  $C_{rel}$  between subspaces  $\mathcal{H}_1$  and  $\mathcal{H}_2$ , indicated by the non-zero off-diagonal elements  $|00\rangle\langle11|$  and  $|11\rangle\langle00|$ .
- It exhibits intra-block structure within each subspace, allowing us to monitor purity changes.
- The eigenvalues  $\lambda_1 = \frac{5}{8}$  and  $\lambda_2 = \lambda_3 = \lambda_4 = \frac{1}{8}$  ensure the state is mixed but not maximally so, allowing coherence to evolve.
- It represents a physically relevant scenario where a quantum system starts with substantial coherence resources that can degrade under noisy operations.

This choice allows clear observation of the coherenceto-noise transformation while preserving mathematical tractability for analytical calculations.

#### Step 3: Calculation of Initial Resource Metrics

(a)  $C_{rel}(\rho, C)$ 

We first compute the block-diagonal state after dephasing:

$$\hat{P}_{1}\rho\hat{P}_{1} = \frac{3}{8}|00\rangle\langle00| + \frac{1}{8}|01\rangle\langle01|,$$

$$\hat{P}_{2}\rho\hat{P}_{2} = \frac{1}{8}|10\rangle\langle10| + \frac{3}{8}|11\rangle\langle11|.$$
(26)

Using the definition:

$$C_{\rm rel}(\rho, \mathcal{C}) = S(\Delta[\rho]) - S(\rho). \tag{27}$$

Since

$$\Delta[\rho] = \hat{P}_1 \rho \hat{P}_1 + \hat{P}_2 \rho \hat{P}_2 
= \frac{3}{8} |00\rangle \langle 00| + \frac{1}{8} |01\rangle \langle 01| + \frac{1}{8} |10\rangle \langle 10| 
+ \frac{3}{8} |11\rangle \langle 11|,$$
(28)

therefore,

$$S(\rho) = -\frac{5}{8} \log_2 \frac{5}{8} - \frac{3}{8} \log_2 \frac{1}{8},$$

$$S(\Delta[\rho]) = -\frac{3}{4} \log_2 \frac{3}{8} - \frac{1}{4} \log_2 \frac{1}{8}.$$
(29)

We have

$$C_{\text{rel}}(\rho, \mathcal{C}) = -\frac{3}{4}\log_2\frac{3}{8} + \frac{5}{8}\log_2\frac{5}{8} + \frac{1}{8}\log_2\frac{1}{8}.$$
 (30)

#### (b) intra-block noise $\mathcal{D}_{rel}(\rho)$

We compute the conditional states within each subspace and their deviation from maximally mixed state:

$$\rho_{1} = \frac{\hat{P}_{1}\rho\hat{P}_{1}}{p_{1}} = \frac{3}{4}|00\rangle\langle00| + \frac{1}{4}|01\rangle\langle01|,$$

$$\rho_{2} = \frac{\hat{P}_{2}\rho\hat{P}_{2}}{p_{2}} = \frac{1}{4}|10\rangle\langle10| + \frac{3}{4}|11\rangle\langle11|.$$
(31)

Calculate the relative entropy:

$$D[\rho_1 \mid\mid \kappa_1] = \text{Tr}[\rho_1(\log_2 \rho_1 - \log_2 \kappa_1)]$$

$$= \frac{3}{4}\log_2 3 - 1,$$

$$D[\rho_2 \mid\mid \kappa_2] = \text{Tr}[\rho_2(\log_2 \rho_2 - \log_2 \kappa_2)]$$

$$= \frac{3}{4}\log_2 3 - 1.$$
(32)

For  $p_1 = p_2 = \frac{1}{2}$ ,

$$\mathcal{D}_{\text{rel}}(\rho) = \sum_{x} p_x D[\rho_x \mid\mid \kappa_x] = \frac{3}{4} \log_2 3 - 1.$$
 (33)

#### (c) Total Inconsistency

$$\mathcal{O}_{\mathcal{C}}(\rho) = \mathcal{C}_{\text{rel}}(\rho, \mathcal{C}) + \mathcal{D}_{\text{rel}}(\rho)$$

$$= -\frac{3}{4}\log_2\frac{3}{8} + \frac{5}{8}\log_2\frac{5}{8}$$

$$+\frac{1}{8}\log_2\frac{1}{8} + \frac{3}{4}\log_23 - 1.$$
(34)

### Step 4: Construction of the Degradation Channel

The free operation is defined as:

$$\Lambda_{\varepsilon}(\rho) = (1 - \varepsilon)\rho + \varepsilon |00\rangle\langle 00|, \tag{35}$$

where  $0 \le \varepsilon \le 1$ .

- Why is it a free operation? This operation probabilistically replaces the state with a fixed block-diagonal state  $|00\rangle\langle00|$ . In the resource theory of block coherence, operations that can prepare or introduce BI states are typically considered free, as they cannot create  $\mathcal{C}_{\rm rel}$ . This channel is a convex combination of such preparation operations and is thus free.
- Why choose this operation? This channel is simple in design yet clearly demonstrates the degradation mechanism. By resetting the system to a specific pure state (which is block-diagonal under the chosen coarse-graining) with probability  $\varepsilon$ , it directly reduces the coherence between different blocks ( $\Delta C_{\rm rel} < 0$ ). Simultaneously, because the reset state is pure, it possesses high purity within its own block, increasing the  $\mathcal{D}_{\rm rel}$  ( $\Delta \mathcal{D}_{\rm rel} > 0$ ). By tuning  $\varepsilon$ , the degree of degradation can be controlled, enabling verification that  $\Delta \mathcal{O}_{\mathcal{C}} \approx 0$  holds for specific parameters.

After this operation acts on the initial state  $\rho$ , we have

$$\Lambda_{\varepsilon}(\rho) = \frac{3+5\varepsilon}{8} |00\rangle\langle00| + \frac{1-\varepsilon}{4} |00\rangle\langle11| 
+ \frac{1-\varepsilon}{8} |01\rangle\langle01| + \frac{1-\varepsilon}{8} |10\rangle\langle10| 
+ \frac{1-\varepsilon}{4} |11\rangle\langle00| + \frac{3-3\varepsilon}{8} |11\rangle\langle11|,$$
(36)

where the eigenvalues of  $\Lambda_{\varepsilon}(\rho)$  are  $\lambda_1^{\varepsilon} = \lambda_2^{\varepsilon} = \frac{1-\varepsilon}{8}$  and  $\lambda_3^{\varepsilon} = \frac{3+\varepsilon-2\sqrt{5}\varepsilon^2-2\varepsilon+1}{8}$ ,  $\lambda_4^{\varepsilon} = \frac{3+\varepsilon+2\sqrt{5}\varepsilon^2-2\varepsilon+1}{8}$ .

## Step 5: Calculation of Final Resource Metrics (a) $C_{\mathbf{rel}}(\Lambda_{\varepsilon}(\rho), \mathcal{C})$

Calculate the projected states:

$$\hat{P}_{1}\Lambda_{\varepsilon}(\rho)\hat{P}_{1} = \frac{3+5\varepsilon}{8}|00\rangle\langle00| + \frac{1-\varepsilon}{8}|01\rangle\langle01|,$$

$$\hat{P}_{2}\Lambda_{\varepsilon}(\rho)\hat{P}_{2} = \frac{1-\varepsilon}{8}|10\rangle\langle10| + \frac{3-3\varepsilon}{8}|11\rangle\langle11|.$$
(37)

Using the definition:

$$C_{\rm rel}(\Lambda_{\varepsilon}(\rho), \mathcal{C}) = S(\Delta[\Lambda_{\varepsilon}(\rho)]) - S(\Lambda_{\varepsilon}(\rho)). \tag{38}$$

Since

$$\Delta[\Lambda_{\varepsilon}(\rho)] = \hat{P}_{1}\Lambda_{\varepsilon}(\rho)\hat{P}_{1} + \hat{P}_{2}\Lambda_{\varepsilon}(\rho)\hat{P}_{2} 
= \frac{3+5\varepsilon}{8}|00\rangle\langle00| + \frac{1-\varepsilon}{8}|01\rangle\langle01| 
+ \frac{1-\varepsilon}{8}|10\rangle\langle10| + \frac{3-3\varepsilon}{8}|11\rangle\langle11|,$$
(39)

therefore,

$$S(\Lambda_{\varepsilon}(\rho)) = -\frac{1-\varepsilon}{4}\log_2\frac{1-\varepsilon}{8} -\lambda_3^{\varepsilon}\log_2\lambda_3^{\varepsilon} -\lambda_4^{\varepsilon}\log_2\lambda_4^{\varepsilon},$$

$$(40)$$

$$S(\Delta[\Lambda_{\varepsilon}(\rho)]) = -\frac{3+5\varepsilon}{8}\log_2\frac{3+5\varepsilon}{8} -\frac{1-\varepsilon}{4}\log_2\frac{1-\varepsilon}{8} -\frac{3-3\varepsilon}{8}\log_2\frac{3-3\varepsilon}{8}.$$
(41)

Then.

$$C_{\text{rel}}(\Lambda_{\varepsilon}(\rho), \mathcal{C}) = -\frac{3 - 3\varepsilon}{8} \log_2 \frac{3 - 3\varepsilon}{8} -\frac{3 + 5\varepsilon}{8} \log_2 \frac{3 + 5\varepsilon}{8} + \lambda_4^{\varepsilon} \log_2 \lambda_4^{\varepsilon} + \lambda_4^{\varepsilon} \log_2 \lambda_4^{\varepsilon}.$$

$$(42)$$

(b) intra-block noise  $\sum\limits_{x}p_{x}^{\varepsilon}D[\rho_{x}^{\varepsilon}\mid\mid\kappa_{x}]$ 

For  $p_1^{\varepsilon} = \frac{1+\varepsilon}{2}$ ,  $p_2^{\varepsilon} = \frac{1-\varepsilon}{2}$ , one can verify that:

$$\begin{split} \rho_{1}^{\varepsilon} &= \frac{\hat{P}_{1} \Lambda_{\varepsilon}(\rho) \hat{P}_{1}}{p_{1}^{\varepsilon}} \\ &= \frac{3 + 5\varepsilon}{4(1 + \varepsilon)} |00\rangle\langle 00| + \frac{1 - \varepsilon}{4 + 4\varepsilon} |01\rangle\langle 01|, \\ \rho_{2}^{\varepsilon} &= \frac{\hat{P}_{2} \Lambda_{\varepsilon}(\rho) \hat{P}_{2}}{p_{2}^{\varepsilon}} \\ &= \frac{1}{4} |10\rangle\langle 10| + \frac{3}{4} |11\rangle\langle 11|. \end{split} \tag{43}$$

Calculate the quantum relative entropy:

$$D[\rho_1^{\varepsilon} \mid\mid \kappa_1] = \text{Tr}[\rho_1^{\varepsilon}(\log_2 \rho_1^{\varepsilon} - \log_2 \kappa_1)]$$

$$= \frac{3 + 5\varepsilon}{4(1 + \varepsilon)} \log_2 \frac{3 + 5\varepsilon}{4(1 + \varepsilon)}$$

$$+ \frac{1 - \varepsilon}{4(1 + \varepsilon)} \log_2 \frac{1 - \varepsilon}{4(1 + \varepsilon)} + 1,$$

$$D[\rho_2^{\varepsilon} \mid\mid \kappa_2] = \frac{3}{4} \log_2 3 - 1,$$
(44)

then

$$\mathcal{D}_{\text{rel}}(\Lambda_{\varepsilon}(\rho)) = \frac{3+5\varepsilon}{8} \log_2 \frac{3+5\varepsilon}{4(1+\varepsilon)} + \frac{1-\varepsilon}{8} \log_2 \frac{27(1-\varepsilon)}{4(1+\varepsilon)} + \varepsilon.$$
(45)

(c) Total Inconsistency  $\mathcal{O}_{\mathcal{C}}(\Lambda_{\varepsilon}(\rho))$ 

$$\mathcal{O}_{\mathcal{C}}(\Lambda_{\varepsilon}(\rho)) = \mathcal{C}_{\text{rel}}(\Lambda_{\varepsilon}(\rho), \mathcal{C}) + \mathcal{D}_{\text{rel}}(\Lambda_{\varepsilon}(\rho))$$

$$= \lambda_{3}^{\varepsilon} \log_{2} \lambda_{3}^{\varepsilon} - \frac{3 + 5\varepsilon}{8} \log_{2} \frac{1 + \varepsilon}{2}$$

$$- \frac{3 - 3\varepsilon}{8} \log_{2} \frac{1 - \varepsilon}{8} + \lambda_{4}^{\varepsilon} \log_{2} \lambda_{4}^{\varepsilon}$$

$$+ \frac{1 - \varepsilon}{8} \log_{2} \frac{1 - \varepsilon}{4 + 4\varepsilon} + \varepsilon.$$
(46)

### Step 6: Degradation Analysis

For  $\varepsilon = 0.26$ , we obtain the following results:

$$\Delta C_{\rm rel} = C_{\rm rel}(\Lambda_{\varepsilon}(\rho), \mathcal{C}) - C_{\rm rel}(\rho, \mathcal{C}) \approx -0.12986, 
\Delta D_{\rm rel} = D_{\rm rel}(\Lambda_{\varepsilon}(\rho)) - D_{\rm rel}(\rho) \approx 0.12898, 
\Delta \mathcal{O}_{\mathcal{C}} = \mathcal{O}_{\mathcal{C}}(\Lambda_{\varepsilon}(\rho)) - \mathcal{O}_{\mathcal{C}}(\rho) \approx -0.00089, 
\eta(\rho) \approx 0.58174, \quad \eta(\Lambda_{\varepsilon}(\rho)) \approx 0.29450, 
\mathcal{O}_{\mathcal{C}}(\rho) \approx 0.45121, \quad \frac{|\Delta C_{\rm rel}|}{\mathcal{O}_{\mathcal{C}}(\rho)} \approx 0.28735.$$
(47)

These results satisfy the following conditions:

$$\Delta C_{\rm rel} < 0, \quad \Delta D_{\rm rel} > 0, \quad |\Delta D_{\rm rel}| \approx |\Delta C_{\rm rel}|,$$

$$\Delta O_{\mathcal{C}} \approx 0, \quad \eta(\Lambda_{\varepsilon}(\rho)) \approx \eta(\rho) - \frac{|\Delta C_{\rm rel}|}{O_{\mathcal{C}}(\rho)}.$$
(48)

We observe that  $\Delta \eta \approx 0.28724$ , indicating a significant decline in quantum resource quality—i.e., notable resource degradation under the influence of the free operation  $\Lambda_{\varepsilon}$ . Meanwhile,  $\Delta \mathcal{O}_{\mathcal{C}} \approx 0$  suggests that the total amount of resources remains almost unchanged. These findings are consistent with our theory.

#### References

- J. Åberg, Quantifying superposition, arXiv:quant-ph/06 12146 (2008).
- T. Baumgratz, M. Cramer, and M. B. Plenio, Quantifying coherence, Phys. Rev. Lett. 113, 140401 (2014).
- F. Bischof, H. Kampermann, and D. Bruß, Resource theory of coherence based on positive - operator - valued measures, Phys. Rev. Lett. 123, 110402 (2019).
- J. W. Xu, L. H. Shao, and S. M. Fei, Coherence measures with respect to general quantum measurements, Phys. Rev. A 102, 012411 (2020).
- S. Kim, C. H. Xiong, A. Kumar, G. J. Zhang, and J. D. Wu, Quantifying dynamical coherence with coherence measures, Phys. Rev. A 104, 012404 (2021).
- A. E. Rastegin, Quantum coherence quantifiers based on the Tsallis relative entropies, Phys. Rev. A 93, 032136 (2016).
- D. Šafránek, J. M. Deutsch, and A. Aguirre, Quantum coarse - grained entropy and thermodynamics, Phys. Rev. A 99, 010101 (2019).
- 8. D. Šafránek, J. M. Deutsch, and A. Aguirre, Quantum coarse grained entropy and thermalization in closed systems, Phys. Rev. A 99, 012103 (2019).
- D. Šafránek, A. Aguirre, J. Schindler, and J. M. Deutsch A brief introduction to observational entropy, Found. Phys. 51, 101 (2021).
- J. Schindler, D. Šafránek, and A. Aguirre, Quantum correlation entropy, Phys. Rev. A 102, 052407 (2020).
- P. Strasberg, and A. Winter, First and second law of quantum thermodynamics: a Consistent derivation based on a microscopic definition of entropy, Phys. Rev. X 2, 030202 (2021).
- 12. X. Zhou, and Z. J. Zheng, Relations between the quantum correlation entropy and quantum discord for X states in multipartite systems, Eur. Phys. J. Plus 137, 625 (2022).

- X. Zhou, and Z. J. Zheng, Relations between the observational entropy and Rényi information measures, Quantum Inf. Process 137, 625 (2022).
- X. Zhou, Relations between observational entropy and other measures based on Tsallis - q entropy, Int. J. Theor. Phys. 62, 12 (2023).
- X. Zhou, Dynamical behavior of quantum correlation entropy under the noisy quantum channel for multiqubit systems. Int. J. Theor. Phys. 62, 23 (2023).
- X. Zhou, Superposition measures with respect to coarsegrained measurement in the generalized n - qubit Werner state. Quantum Inf. Process 22, 156 (2023).
- F. Buscemi, J. C. Schindler, D. Šafránek, Observational entropy, coarse - grained states, and the Petz recovery map: information - theoretic properties and bounds, New J. Phys. 25 053002 (2023).
- G. Bai, D. Šafránek, J. Schindler, F. Buscemi, and V. Scarani, Observational entropy with general quantum priors, Quantum 8, 1524 (2024).
- J.R. McClean, S. Boixo, V.N. Smelyanskiy, et al. Barren plateaus in quantum neural network training landscapes. Nat. Commun. 9, 4812 (2018).
- M. Cerezo, A. Arrasmith, R. Babbush, et al. Variational quantum algorithms. Nat. Rev. Phys. 3, 625 - 644 (2021).
- M. Iman and W.S. Robert, The theory of manipulations of pure state asymmetry: I. Basic tools, equivalence classes and single copy transformations, 2013 New J. Phys. 15 033001.
- 22. I. Marvian, R. Spekkens, Extending Noether's theorem by quantifying the asymmetry of quantum states. Nat. Commun. 5, 3821 (2014).
- G. Gour, I. Marvian , and R. W. Spekkens. Measuring the quality of a quantum reference frame: the relative entropy of frameness, Phys. Rev. A 80. 012307(2009).
- I. Marvian, R.W. Spekkens, and P. Zanardi, Quantum speed limits, coherence, and asymmetry, Phys. Rev. A 93. 052331(2016).
- I. Marvian and R. W. Spekkens, How to quantify coherence: Distinguishing speakable and unspeakable notions, Phys. Rev. A 94, 052324(2016).
- S. Sachdev, Quantum phase transitions. 2nd ed. Cambridge University Press 2011.
- Z. Holmes, K. Sharma, M. Cerezo, & Coles, P. J., Connecting ansatz expressibility to gradient magnitudes and barren plateaus, PRX Quantum, 3(1), 010313.
- S. Wang, E. Fontana, M. Cerezo, et al. Noise induced barren plateaus in variational quantum algorithms. Nat. Commun. 12, 6961 (2021).